Cell. Mol. Life Sci. 65 (2008) 324 – 337
1420-682X/08/020324-14
DOI 10.1007/s00018-007-7499-7

Cellular and Molecular Life Sciences

Research Article

The cytotoxicity of eosinophil cationic protein/ribonuclease 3 on eukaryotic cell lines takes place through its aggregation on the cell membrane

S. Navarro[a], J. Aleu[b], M. Jiménez[b], E. Boix[a], C. M. Cuchillo[a] and M. V. Nogués[a,*]

[a] Departament de Bioquímica i Biologia Molecular, Facultat de Biociències, Universitat Autònoma de Barcelona, 08193 Bellaterra (Spain), Fax: +34-93-5811264, e-mail: victoria.nogues@uab.cat
[b] Departament de Biologia Cellular, de Fisiologia i d'Immunologia, Facultat de Veterinària, Universitat Autònoma de Barcelona, 08193 Bellaterra (Spain)

Received 26 October 2007; accepted 23 November 2007
Online First 18 December 2007

Abstract. Human eosinophil cationic protein (ECP)/ribonuclease 3 (RNase 3) is a protein secreted from the secondary granules of activated eosinophils. Specific properties of ECP contribute to its cytotoxic activities associated with defense mechanisms. In this work the ECP cytotoxic activity on eukaryotic cell lines is analyzed. The ECP effects begin with its binding and aggregation to the cell surface, altering the cell membrane permeability and modifying the cell ionic equilibrium. No internalization of the protein is observed. These signals induce cell-specific morphological and biochemical changes such as chromatin condensation, reversion of membrane asymmetry, reactive oxygen species production and activation of caspase-3-like activity and, eventually, cell death. However, the ribonuclease activity component of ECP is not involved in this process as no RNA degradation is observed. In summary, the cytotoxic effect of ECP is attained through a mechanism different from that of other cytotoxic RNases and may be related with the ECP accumulation associated with the inflammatory processes, in which eosinophils are present.

Keywords. Eosinophil cationic protein, ribonuclease, eukaryotic cell cytotoxicity, protein aggregation, cell membrane binding.

Introduction

Human eosinophil cationic protein (ECP)/ribonuclease 3 (RNase 3) is a protein secreted from the secondary granules of the activated eosinophils. ECP is a polypeptide with a molecular mass of 15.5 kDa, although glycosylated forms with molecular masses ranging from 18 to 22 kDa are also found. The amino acid sequence and the three-dimensional structure show that ECP is a member of the ribonuclease A superfamily, a vertebrate-specific enzyme family that includes eight human proteins that conserve the same active site amino acid residues. A well-known enzyme, the non-glycosylated bovine pancreatic ribonuclease A (RNase A) is the archetype of this protein family. ECP shows a 30% sequence homology with the human pancreatic form (RNase 1) and it shares a 67% of sequence identity with the eosinophil-derived neurotoxin (EDN)/RNase 2. EDN is another member

* Corresponding author.

of this protein family that is also found in human eosinophils. The RNase activity of ECP is 100-fold lower than that of RNase A and 10-fold lower than that of EDN [1, 2]. Interestingly, some specific properties of ECP rely on its cytotoxicity, which is associated with important defense mechanisms; thus, ECP shows bactericidal [3], helminthotoxic [4, 5] and antiviral activities [6]. In addition, important extracellular deposits of ECP are found in tissues undergoing eosinophilic inflammation and they correlate well with tissue damage as it happens, for example, in the case of bronchial asthma or in the intestinal mucosa as is the case in Crohn's disease [7]. ECP levels in body fluids are currently used as marker of eosinophil activity and turnover, and correlate well with tissue damage [8]. After intraventricular injection into guinea pigs and rabbits, ECP causes the Gordon phenomenon that is characterized by cerebellar Purkinje cell degeneration [9]. Cytotoxic effects of ECP have also been described for different mammalian cell lines [10, 11]. Although the molecular basis of the ECP effect on eukaryotic cells remains unknown, it has been described that ECP forms voltage-insensitive and non-selective transmembrane pores, and it has been suggested that this could be the basis of the mechanism for cell killing [12]. The high number of arginine residues on the molecular surface and the tryptophan residue at position 35 are crucial to the cytotoxic activity of ECP, which suggests that these residues contribute to the destabilization of the phospholipid bilayer [11, 13]. In addition, recent studies have demonstrated that glycosylation affects neither the cytotoxic nor the RNase activities of native ECP [14].

Two proteins of the RNase A superfamily, bovine seminal ribonuclease (BS-RNase) and onconase (ONC) are potent cytotoxins that have been extensively characterized [15]. BS-RNase, obtained from bovine sperm, is a dimeric protein with two identical subunits; it shows aspermatogenic, antitumor, embryotoxic and immunosuppressive activities. The cytotoxic effect of BS-RNase is accompanied by the induction of apoptosis both in human lymphocytes and in several tumor cell lines [16, 17]; it enters into the cells by adsorptive endocytosis and evades the cytosolic ribonuclease inhibitor [18]. ONC is an RNase isolated from amphibian oocytes, and is cytostatic and cytotoxic to numerous tumor cell lines [19]. The tumor growth -controlling effect of ONC is achieved by degrading RNA within cancer cells. This results in the inhibition of protein synthesis and the arrest of the cell cycle in the G_0/G_1 phase [20]. ONC-treated cell lines also displayed apoptosis [21] and, recently, an unusual entry process that relies on clathrin-dependent endocytic uptake has been described [22]. Recent studies indicate that ONC substantially decreases the content of reactive oxygen species (ROS) both in normal and in tumor cell lines [23].

Apoptosis and necrosis are two forms of cell death that have been defined on the basis of distinguishable morphological criteria [24, 25], even if they may involve several common signaling and execution mechanisms. In fact, recent evidence suggests that identical initiation signals can be involved both in apoptotic and in necrotic cell death [25].

In an effort to understand the cytotoxic mechanism of ECP on mammalian cells we have analyzed its cellular effects using HL-60 and HeLa cell lines as models. In this work we have demonstrated that the effect of ECP is achieved through a mechanism different to that of other cytotoxic RNases; the observations show a direct relationship between cytotoxicity and the ECP accumulation associated to inflammatory processes. The ECP cytotoxic effects begin with the binding and aggregation of the protein to the cell surface. This is followed by an alteration of the cell membrane permeability, which results in a modification of the ionic intracellular equilibrium. These signals initiate specific morphological and biochemical cellular changes such as chromatin condensation, reversion of membrane asymmetry, ROS production, activation of caspase-3-like activity and, eventually, cell death. In contrast with other cytotoxic RNases no internalization of the protein is observed.

Materials and methods

Preparation of recombinant ECP

A human ECP synthetic gene was used to obtain recombinant ECP. The protein was expressed in *E. coli* BL21 (DE3) strain (Novagen, USA) using the pET11c expression vector and was purified from inclusion bodies [1]. In all the experiments, diluted protein samples were centrifuged at 9000 *g* for 10 min before use.

Cell culture conditions

Human acute promyelocytic leukemia cell line HL-60 [CCL-240, American Type Culture Collection (ATCC), USA] was maintained in continuous suspension culture in RPMI 1640 medium (Vitacell, USA), containing 10 mM HEPES, 1 mM sodium pyruvate, 2 mM L-glutamine, 4.5 g/L glucose and 1.5 g/L sodium bicarbonate; the cervix HeLa adenocarcinoma cell line (CCL-2, ATCC) was maintained in Dulbecco's Modified Eagle's medium (DMEM; Vitacell). Both media were supplemented with 10% heat-inactivated fetal calf serum (FCS), 200 U/mL penicillin and 0.2 mg/mL streptomycin, and cells were

incubated at 37 °C under moisturized air containing 5 % CO_2.

Cell growth and viability assay

Metabolic cell activity was determined with the Cell Proliferation kit I (MTT; Roche, USA), a colorimetric assay based on the cleavage of the yellow 3-[4,5-dimethylthiazol-2-yl]-2,5-diphenyl tetrazolium bromide salt (MTT) to purple formazan crystals. Exponentially growing HL-60 (2×10^5 cell/mL) and HeLa cell cultures (5×10^4 cells/well, serum-depleted to 0.5 % FCS for 6 h before ECP treatment) were plated in 96-well dishes (Orange Scientific, Belgium), and treated with ECP concentrations ranging from 10 to 40 μM for 24, 48 and 72 h. Protein samples were diluted in PBS. Positive controls of cell growth were carried out by adding the same volume of PBS without protein. Cell viability was determined following the working instructions provided by Roche and measuring the difference in absorbance between 540 nm and 690 nm. In each set of assays, analyses were carried out in duplicate or triplicate.

This assay was also used to check the effect, at a 50 μM concentration, of benzyloxycarbonyl-aspartyl(OMe)-fluoromethylketone (Boc-Asp-FMK; Calbiochem, UK), a cell-permeable broad-spectrum caspase peptide inhibitor, on the metabolic activity of ECP-treated cells.

Cell morphology

The effect of ECP on cell morphology was analyzed by fluorescence microscopy (Leica DMR8, Germany), using a filter block that included a 515–560-nm excitation filter and a 580-nm emission filter. HL-60 cells (0.5×10^6 cells) were treated with 10 and 20 μM ECP for 24 and 48 h followed by the addition of 10 μg/mL propidium iodide (PI), and were incubated for 30 min. Samples were pelleted by centrifugation, washed in PBS and mounted on glass slides using Fluoprep (Biomérieux, France). Anisomycin (2-p-methoxyphenylmethyl-3-acetoxy-4-hydroxypyrrolidine, 2 μg/mL) was used as a positive control of apoptosis [26].

Conjugation of ECP and RNase A with the Alexa Fluor 488 dye

ECP or RNase A (Sigma Aldrich), 0.5 mL of a 2 mg/mL protein concentration, was labeled using the Alexa Fluor 488 Protein Labeling kit (Molecular Probes, USA) following the instructions of the manufacturer. A PD10-desalting column (GE Healthcare) equilibrated with PBS at pH 7.2 was used to separate labeled protein from free dye.

The degree of labeled protein was calculated as: $m = nA_{494}/71\,000P$ [where m is the mol dye/mol protein, n is the dilution factor, A_{494} the absorbance at 494 nm and P the protein concentration (M)].

Confocal microscopy

Experiments were carried out in complete culture medium, at 37 °C and in a 5 % CO_2 atmosphere. HeLa cells were seeded in 35-cm^2 plates with a glass coverslip and grown to about 80 % confluence prior to experiments. Cell viability was assessed by incubating the cells in the presence of 5 μg/mL Alexa Fluor 568-transferrin (Molecular Probes) for 40 min; the cells were then washed with PBS buffer three times to eliminate the fluorescent marker and finally complete medium sufficient to cover the surface of the plate was added. Alexa Fluor 488-ECP (2 μM) was added directly to the cultures and time lapse was recorded at intervals of 2 min in short-term (0–35 min) experiments and of 10 min in long-term (3–8 h) experiments.

For the colocalization experiments, 5 μL 1 mM Vibrant DiI cell-labeling solution (Molecular Probes) were added to 1 mL of complete growth medium. Cells were incubated at 37 °C for 10 min and washed with PBS buffer three times. For each wash cycle, cells were washed with PBS then covered with fresh medium and incubated for 10 min.

Confocal images of the cultures were captured using a laser scanning confocal microscope (Leica TCS SP2 AOBS equipped with a HCX PL APO 63x1.4 oil immersion objective, Germany). The Alexa Fluor 488-ECP images were acquired using a 488-nm argon laser (515–540 nm emission collected). Both Vibrant DiI and Alexa Fluor 568-transferrin were excited using an orange diode (588–715 nm emission collected).

In the time-lapse analysis, xyt (300 μm) sections were captured at each time point in several independent experiments. Similar experiments were carried out using Alexa Fluor 488-RNase A.

Cytosolic free Ca^{2+} and Na^+ concentration assays

HeLa cells were washed, detached with trypsin and reseeded onto glass coverslips 24 h before calcium measurements. Fluo-4/AM (Teflabs, USA) was used to monitor changes of the calcium levels in the cytosol. Fluo-4 was dissolved [50 μg in 25 μl dimethylsulfoxide (DMSO)] and 2 μL of this stock solution was added to each culture plate in 1 mL recording medium (10 mM HEPES, 140 mM NaCl, 4.8 mM KCl, 1 mM $MgCl_2$, 1.8 mM $CaCl_2$ and 10 mM glucose, pH 7.4). After 45-min incubation, the remaining dye was washed out and the cells were incubated in recording medium. For experiments performed in low extracellular calcium concentration, cells were bathed for 10 min in 10 mM HEPES, 140 mM NaCl, 4.8 mM KCl, 2.3 mM $MgCl_2$,

0.5 mM $CdCl_2$, and 10 mM glucose, pH 7.4. An IX-FLA equipment (Olympus Biosystems connected to an Olympus IX70 microscope with a ×20 lens) was used to image the cells. The cells were scanned using Cell® software (Olympus Biosystems). Changes in the Fluo-4 fluorescence were recorded for a 60-s test at 2.5 Hz with a spatial resolution of 512 × 480 pixels and then 20 μM ECP was added. At the end of the experiments the images were analyzed over time, using regions of interest (ROIs). ΔF/F analysis was performed and plotted over time.

Statistical analysis was carried out using the Sigma Stat software (SPSS). Values given in the text correspond to the mean ± SEM. When comparing two-group means of normally distributed data, the Student's *t*-test was used. A significance level of $p < 0.05$ was adopted in all comparisons.

Sodium Green tetraacetate (Molecular Probes) was used to monitor changes in the sodium levels in the cytosol of HeLa cells. Sodium Green was dissolved in DMSO and was added at a 3 μM final concentration in 1 mL recording medium (10 mM HEPES, 4.8 mM KCl and 140 mM NaCl, pH 7.4). Control and 50 μM ECP-treated cells were incubated for 60 min at 37 °C and then washed with PBS to remove excess probe. Changes in the Sodium Green fluorescence were recorded with a laser scanning confocal microscope Leica TCS SP2 AOBS. At the end of the experiments the images were analyzed over time, using ROIs. ΔF/F analysis was carried out and plotted over time.

Flow cytometry techniques

Samples were analyzed on a FACSCalibur cytometer (Becton Dickinson, USA). The instrument was set up with the standard configuration: excitation of the sample was done using a 488-nm air cooled argon-ion laser at 15 mW power. CellQuest software (Becton Dickinson) was used to control the system and to carry out data analysis.

Cell cycle analysis. Cell cycle analysis was performed on HL-60 and HeLa cells ($1 \times 10^6 - 2 \times 10^6$ cells/mL). ECP-treated (20 μM ECP for 24 and 48 h) and control cells were washed with PBS and fixed in ice-cold 70 % ethanol. The slides were washed twice with PBS and incubated with 100 μL 100 μg/mL RNase A (DNase free) for 5 min at room temperature. Then 400 μL 50 μg/mL PI in 3.8 mM sodium citrate were added. Fluorescence intensity was measured at 585/42-nm band pass filter. Data were analyzed with the ModFit LT cell cycle analysis software (Verity Software House, USA). The Student's *t*-test was used to estimate the significance of the values determined for ECP-treated cells with respect to those of non-treated cells. A significance level of $p < 0.05$ was adopted in all comparisons.

Phosphatidylserine exposure assay. HL-60 and HeLa cells (1×10^6 cells/mL) were incubated with 20 μM ECP for 10 and 24 h. HL-60 cells were harvested by centrifugation and HeLa cells were trypsinized prior to centrifugation. Cells were then washed twice with cold PBS and resuspended in 100 μL annexin V-binding buffer (10 mM HEPES-NaOH, 140 mM NaCl and 2.5 mM $CaCl_2$, pH 7.4). Then 5 μL 0.5 nM of annexin V-fluorescein isothiocyanate (annexin V-FITC; Molecular Probes, Invitrogen) and 2 μL 10 mg/mL PI were added. Cells were incubated at room temperature for 15 min, 400 μL annexin V-binding buffer were added and samples were kept on ice in the dark prior to analysis. A 530/30-nm and 585/42 nm-band pass filters were used to measure green fluorescence (annexin staining) and red fluorescence intensity (PI, DNA staining), respectively. Dead cells were excluded by gating population on the FSC (forward scatter) *versus* SSC (side scatter) dot plots. The effect of 2 μg/mL anisomycin for 24 h was used as positive control.

Assay for intracellular ROS generation. HL-60 and HeLa cells (1×10^6 cells/mL) were treated with 20 μM ECP for 24 h. HL-60 cells were harvested by centrifugation and HeLa cells were trypsinized prior to centrifugation. ROS in cells were measured using the oxidation-sensitive fluorescence probe dichlorofluorescein diacetate (DCFH-DA) (Fluka, Switzerland). Cells were incubated with 5 μM DFCH-DA for 15 min at 37 °C. The 2′–7′-dichlorofluorescein (DCF) formation was measured using a 530/30-nm band pass filter. The effect of 100 μM hydrogen peroxide for 24 h was used as positive control.

Caspase-3 activity assay

HL-60 and HeLa cells were harvested after a 24-h ECP treatment (20 μM) and washed with PBS. Pellets of at least 1×10^6 cells for each reaction were frozen for later analysis. Caspase-3 activity was measured following the instructions of the EnzChek Caspase-3 Assay kit (Molecular Probes). Fluorescence intensity was measured using a fluorescence microplate reader at 520 nm and, according to the manufacturer instructions, sensitivity was adjusted with a standard curve. To normalize activity values, protein concentration was determined by the Bradford method. The effect of 2 μg/mL anisomycin for 10 h was used as positive control for caspase-3 activation.

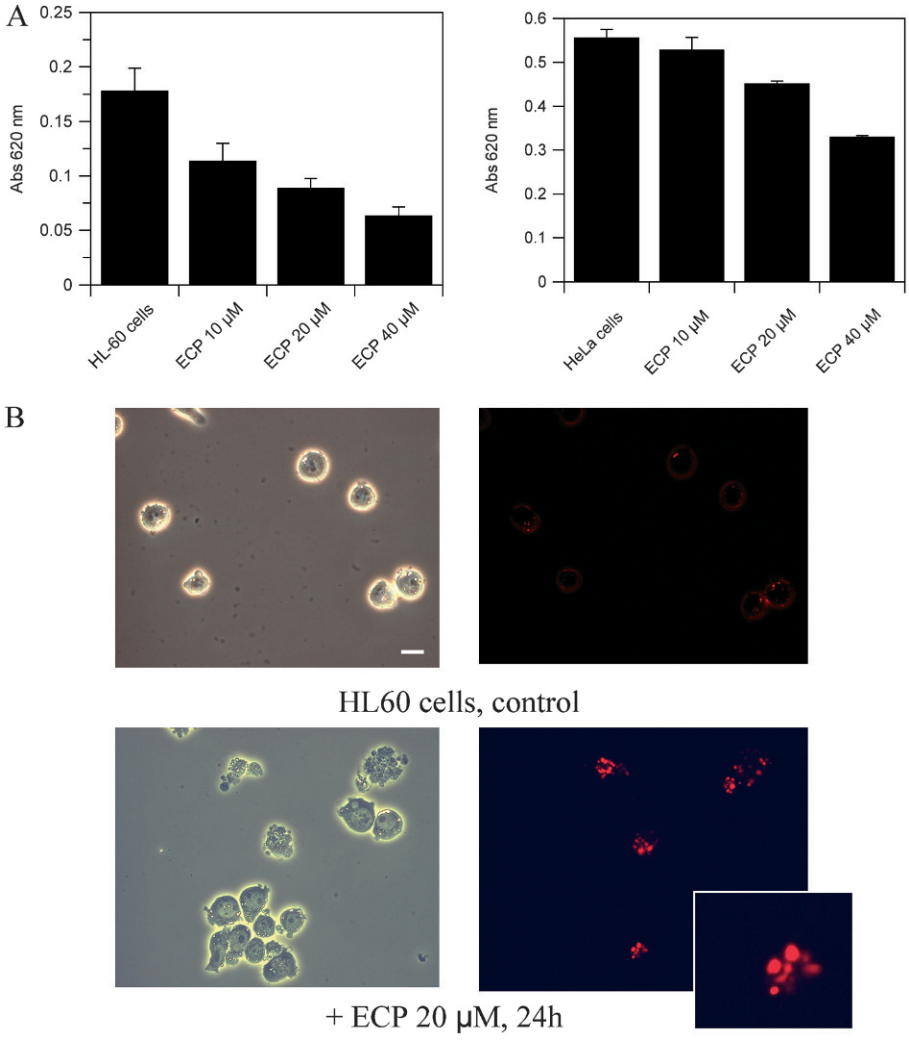

Figure 1. Metabolic and morphological effects of eosinophil cationic protein (ECP) on eukaryotic cell lines. (*A*) Effect of ECP concentration on the metabolic activity of HL-60 and HeLa cells. Control and ECP-treated cell cultures were maintained for 72 h and metabolic activity was determined by the MTT assay. See methods for detailed assay conditions. (*B*) Contrast phase microscopy and fluorescence microscopy by propidium iodide (PI) staining of the ECP effect (20 µM for 24 h) on HL-60 cells. Bar 15 µm.

RNA analysis

HeLa cells (0.5×10^6 cells/mL) cultured in a six-well plate were treated with 20 µM ECP for 24 and 48 h. Cells were processed for RNA isolation using the TRI Reagent® method (Ambion, USA). Cells were homogenized in TRI Reagent (1 mL TRI Reagent/cm^2 cultured dish area), RNA was then extracted with 0.2 volumes of chloroform, precipitated with 0.5 volumes of isopropanol and finally washed with 75% ethanol. RNA was analyzed on an Experion Automated Electrophoresis (Bio-Rad Laboratories, USA). Data were analyzed with the Experion™ Software v1.0 (Bio-Rad).

Results

ECP effect on cell metabolic activity and cell morphology

The effect of ECP on the metabolic activity of suspension cells (HL-60) and adherent cells (HeLa) cultures, as determined by the MTT assay, is shown in Figure 1A; in both cases a dose-dependent effect (from 0 to 40 µM) was observed, although HL-60 cells showed a higher sensitivity than HeLa cells to ECP treatment. In addition, in both cases a time-dependent effect (from 0 to 72 h) was also observed (data not shown). The ECP effect on HL-60 cell morphology was visualized by contrast phase and fluorescence microscopy (Fig. 1B). ECP induces cell aggregation and important changes in cell morphology. The changes in the cell membrane permeability and nuclei morphology can be determined in fresh cultures using fluorescence microscopy and PI staining. ECP-treated cells show intracellular events, e.g., the loss of the plasma membrane integrity and typical apoptotic nuclear morphology changes such as chromatin condensation and apoptotic body formation. This suggests that ECP induces apoptosis in these cell lines. Anisomycin, a protein synthesis inhibitor, was used as control for apoptosis induction. Treatment with 20 µM RNase A under the same conditions neither alters the

metabolic activity nor the cell morphology of HL-60 cell cultures, indicating that RNase A may be used as a negative control for RNase cytotoxicity (data not shown and [11]). Taking into account the ECP cytotoxicity on both HL-60 and HeLa cells as well as the specific requirements of each technique, the following experiments were carried with the most suitable cell line.

Confocal microscopy analysis of ECP dynamic distribution and membrane bilayer colocalization

The ECP distribution on HeLa cell cultures was analyzed using confocal microscopy. Since cell fixation was shown to cause significant artifacts on the cellular localization of proteins [27], distribution of the fluorescent Alexa Fluor 488-ECP was analyzed without fixing cells and maintaining cells cultures at 37 °C in a 5 % CO_2 atmosphere. Alexa Fluor 568-transferrin was used as a culture survival control. The ECP distribution was analyzed in short-term experiments, from 0 to 35 min after ECP addition to the cultures, and in long-term (3–8 h) experiments (Fig. 2A and B, respectively, show some representative images obtained during the time-lapse experiments). The image analysis showed that at a very short time after protein addition (t = 1 min) the labeled ECP was present only in the culture medium; however, a clear binding of the protein and its aggregation on the cell surface was observed in the early stages (35 min). The cell surface binding is maintained both in short-term and long-term experiments, and no internalization of ECP was observed in any case (Fig. 2A and B). Similar experiments using Alexa Fluor 488-RNase A did not show any protein binding (data not shown) in accordance with the results obtained using other experimental approaches, again indicating the lack of cytotoxicity of RNase A. The binding of Vibrant DiI, a marker of membrane phospholipids, to the cell was also analyzed by confocal microscopy. Figure 3 shows the colocalization of ECP and Vibrant DiI. The results of this *"in vivo"* experiments also confirm that ECP is not internalized. Previous studies about the ECP cytotoxicity on eukaryotic cell lines using rhodamine B isothiocyanate (RITC)-labeled ECP and fluorescence microscopy suggested that the protein accumulates in the cytoplasm; however, it was not clear whether endocytosis of ECP had occurred [10]. These contrasting results may be explained by the cell fixation procedure used in the fluorescence microscopy experiments that may promote an artifactual redistribution of the protein into the cell [27].

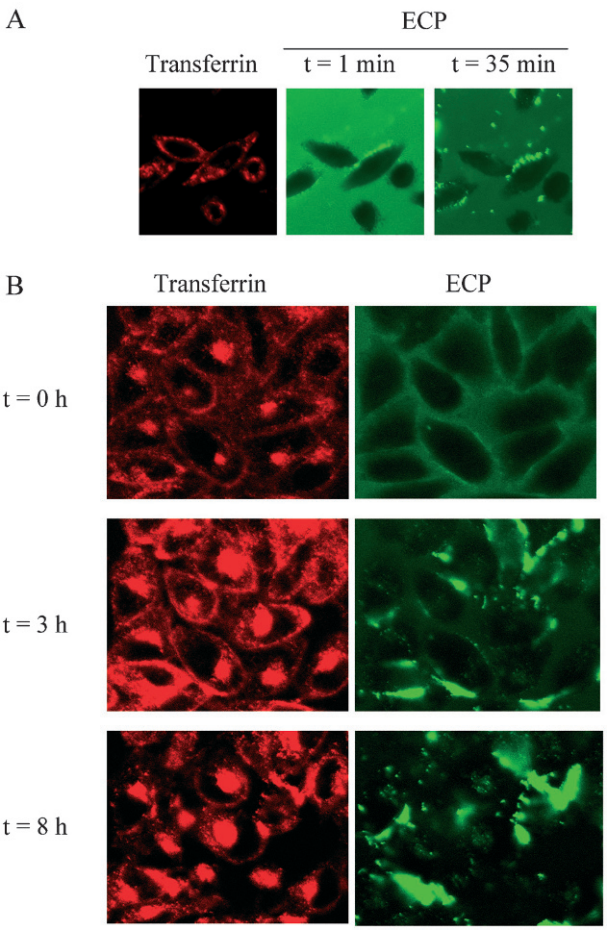

Figure 2. Study of the ECP dynamic distribution on HeLa cell cultures by confocal microscopy. HeLa cells were incubated with medium containing Alexa Fluor 568-transferrin (5 μg/mL), used as a culture survival control, and Alexa Fluor 488-ECP (2 μM). After washing, cells were analyzed by multi-channel confocal microscopy. Images were taken in complete medium at 37 °C and 5 % CO_2 atmosphere. (*A*) Short-term experiments (0–35 min), (*B*) long-term experiments (0–8 h).

The effect of ECP on cell membrane permeability

Fluo-4/AM fluorescent measurements were performed to test whether ECP increases the cytosolic free Ca^{2+} concentration of HeLa cells (Fig. 4). ECP (20 μM) induced a transient cytosolic calcium increase in 60 % of the HeLa cells analyzed (62 out of 104 cells, seven culture wells) in the first 60 s after application of the protein in the recording medium. The amplitude of the cytosolic calcium transient response was 3.7 ± 0.2 times over background level. This effect was dependent on ECP concentration because a 10 μM ECP solution did not induce the transient cytosolic calcium increase (1.21 ± 0.03 U, $n = 15$ cells) (Fig. 4B).

The effect of ECP on HeLa cells was compared with that of RNase A (Fig. 4B). Addition of either 10 or 20 μM RNase A did not induce a cytosolic calcium increase (1.3 ± 0.2 times over background level) in

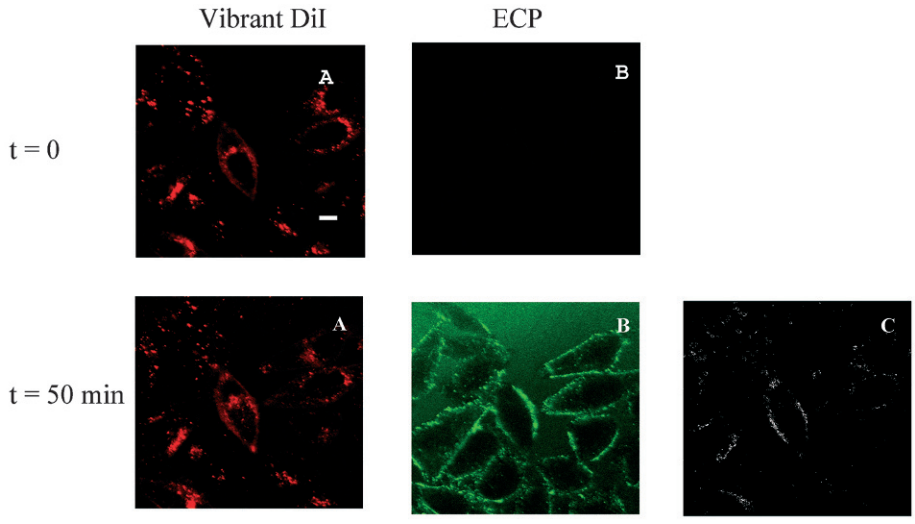

Figure 3. Cellular colocalization of Vibrant DiI and Alexa Fluor 488-ECP on the membrane bilayer of living HeLa cells. Cells were incubated with: *A*, Vibrant DiI solution (1:2000 dilution), a lipophilic membrane stain, for 5 min prior to visualization; and *B*, with Alexa Fluor 488-ECP (2 μM) for 10 min; *C* corresponds to merged images of *A* and *B*. Bar 10 μm.

95% of cells (71 out of 75, from seven culture wells). Only in 5% of the cells was a significant cytosolic calcium increase (3.4 ± 1.7 U) detected.

To elucidate the origin of the calcium that appeared in the cytosol, we carried out some calcium recordings with a low extracellular calcium medium (Fig. 4B). Application of 20 μM ECP in a low-calcium medium did not induce a significant calcium increase in the HeLa cytosol (1.2 ± 0.1 U, $n = 35$ cells, from three culture wells).

An increase of intracellular Na^+ concentration due to the addition of ECP was also detected by changes in the Sodium Green fluorescence detected by confocal microscopy; however, in this case a low signal intensity was obtained (data not shown).

Studies on apoptotic events

Effect of ECP on the cell cycle. The ECP cytotoxicity was also observed in the dot-plot experiments as the increase of dead cells and debris populations of the ECP-treated preparations (see Fig. 5, insets). The DNA content of cells was quantified by flow cytometry of PI staining of permeabilized cells, a method that also allowed the assessment of which phase of the cell cycle the cells were in, as well as monitoring the ECP effect on the dying population (Fig. 5). When the percentage of cells at G_0/G_1, G_2/M and S phase of HL-60 cells in the control and in the presence of 20 μM ECP (Fig. 5) are compared, the results show that the ECP effect was not cell-cycle dependent as judged by the uniform loss of cells from all stages of the cell cycle. The Student's *t*-test was applied considering the difference between cell number averages from three independent experiments and in all cases, the results were not statistically significant as the *p* value was higher than 0.05.

Phosphatidylserine exposure and loss of plasma membrane integrity. The results illustrated in Figure 6 show the effect of ECP on HL-60 cells probed with annexin V-FITC and PI to measure the exposure of phosphatidylserine and plasma membrane permeability. The flip of phosphatidylserine from the inner to the outer leaflet of the plasma membranes by the cleavage of flippase and/or activation of scramblase (floppase) is an early event during the initiation stages of apoptosis [28]. It is possible to determine and differentiate viable, apoptotic and non-viable necrotic cells. On the one hand, the effect of ECP is to increase the debris and dead cells (Fig. 6B, left) and on the other an increase in the percentage of the cell population in apoptotic or necrotic steps is observed when dead cells are excluded by gating (Fig. 6B, right). Anisomycin, a potent apoptotic inductor, was used as positive control. Similar results were obtained in ECP-treated HeLa cells submitted to the same conditions (data not shown).

Intracellular ROS generation. The effect of ECP on the ROS generation of cell cultures (HL-60 and HeLa cells) was determined by flow cytometry using the DCFH-DA assay (Fig. 7). Figure 7A shows the effect of 20 μM ECP for 24 and 48 h on the DCFH fluorescence profile of HL-60 cells. The width-pulse area signal was used to discriminate between G_2 cells and cell doublets and gate out the latter (data not shown). Untreated cells were analyzed to assess the nonspecific oxidation and 10 μM hydrogen peroxide treatment was used as positive control. Figure 7B shows the fluorescence intensity histogram for control and ECP-treated HL-60 and HeLa cells; a significant increase of intracellular ROS generation due to the effect of ECP was observed in both cell types.

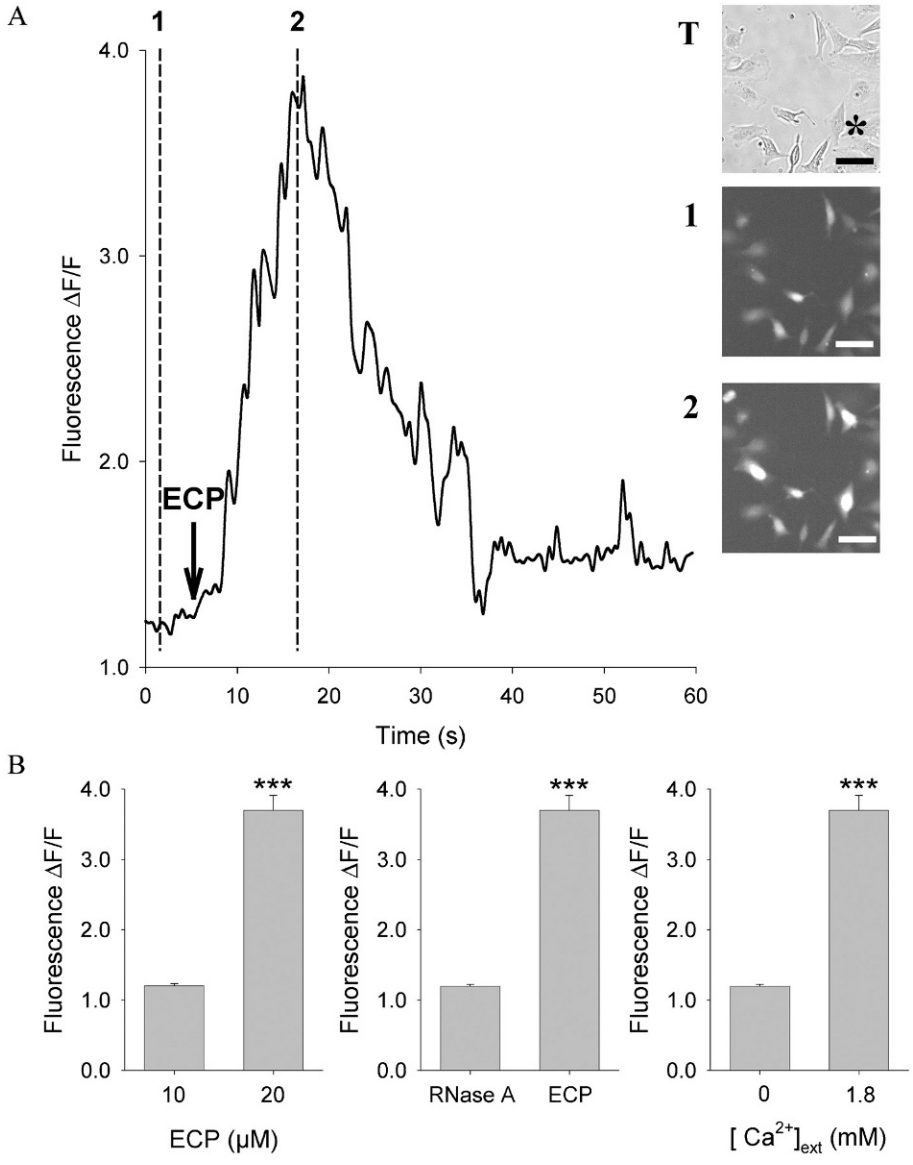

Figure 4. The effect of ECP on HeLa cytosol Ca^{2+} concentration. (*A*) Change in relative Fluo-4 fluorescence (ΔF/F) in one cell (marked with * in transmission microscopy image) in response to the application of 20 μM ECP (shown with an arrow). T, Transmission image, and 1 and 2, images were taken at specific time points corresponding to the dotted lines. Bar 50 μm. (*B*) Average peak amplitude in the Ca^{2+} transients induced by 10 and 20 μM ECP, and by RNase A and ECP (20 μM concentration in each case) all in 1.8 mM extracellular Ca^{2+}, and by 20 μM ECP in low calcium and 1.8 mM calcium media.

Effect of ECP on caspase-3 activity and caspase inhibition

A typical event in apoptotic cell death is activation of the caspase cascade where caspase-3 activity is a critical downstream effector of apoptosis. Caspase-3-like activity was determined with the EnzChek Caspase-3 Assay kit; treatment with 20 μM ECP for 24 h increased the caspase-3 activity in HL-60 and HeLa cells with respect to the control (Fig. 8). Anisomycin was used as positive control for caspase-3 activation [29].

The effect of Boc-Asp-FMK, a caspase activity inhibitor, on the cell metabolic activity of control and ECP-treated HL-60 cells was also assessed with the MTT assay (Table 1). Boc-Asp-FMK is a cell-permeable broad-spectrum caspase peptide inhibitor that irreversibly binds to the protease catalytic site of caspases and inhibits caspase-mediated apoptosis by preventing the processing of caspase proenzymes to their active forms [30]. Caspase inhibition alone increased the cell metabolic activity as a consequence of the inhibition of the residual caspase activity but, in addition, a clear suppression of the ECP effect was also observed.

Effect of ECP on cellular RNA

The contribution of the ribonuclease activity of ECP to its cytotoxic activity was assessed from the analysis of the RNA profiles of control and ECP-treated cells (Fig. 9). No significant RNA breakdown associated to the presence of ECP was observed (lanes 2 and 3). Previous studies also indicated that the ECP intrinsic RNase activity is not necessary for its bactericidal activity [31]. These results may be a consequence of

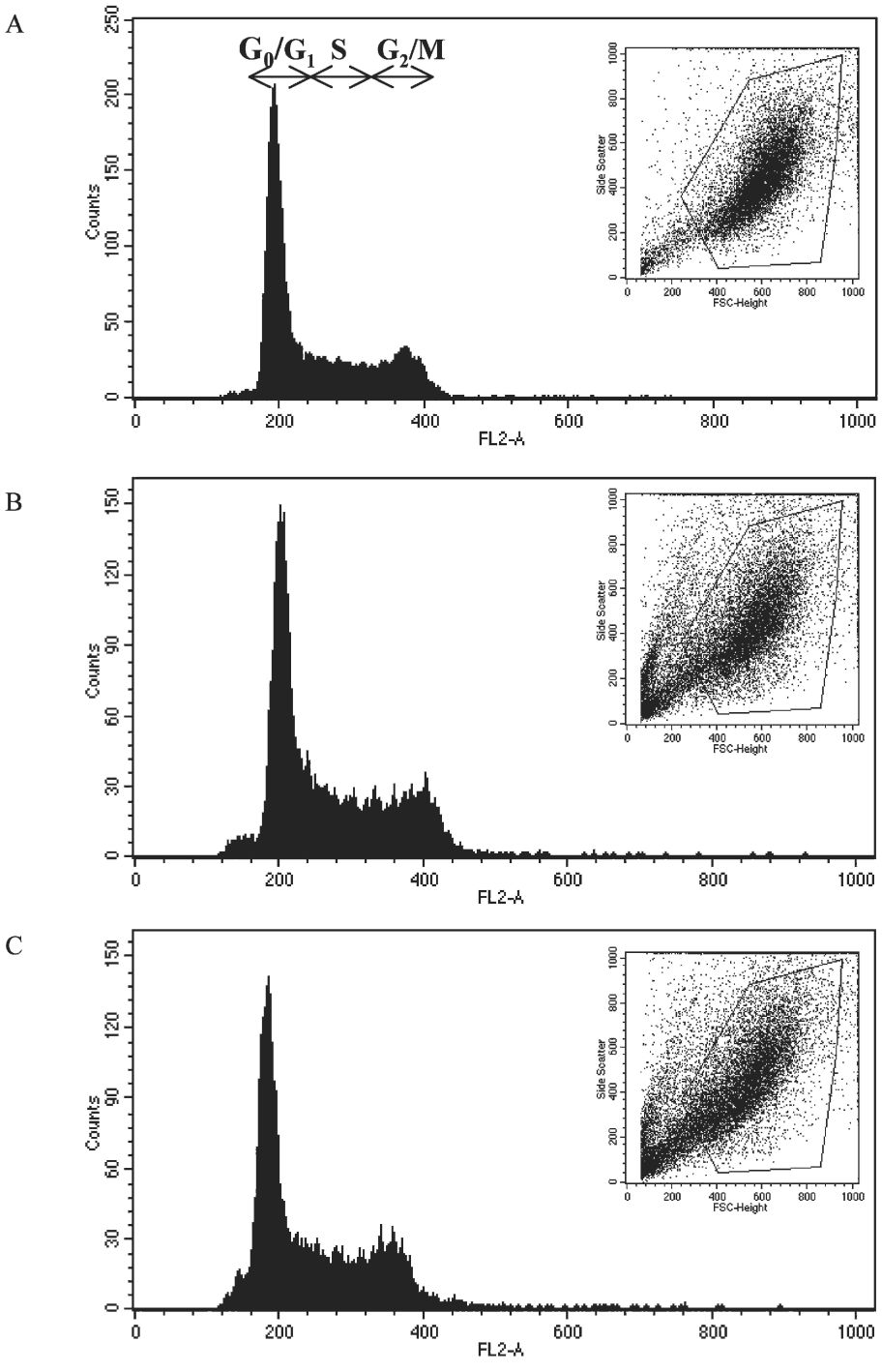

Figure 5. The effect of ECP on time-dependent changes in the cell cycle progression in HL-60 cells. Representative DNA distribution profiles obtained by flow cytometry after cell permeabilization and PI staining of (*A*) untreated cells and (*B*, *C*) 20 μM ECP treated cells for 24 and 48 h, respectively. Dead cells and debris were excluded by gating population on a SSC-H-side scatter *versus* FSC-H-height dot plot (see insets) and cell doublets were gated out by a FL2-A *versus* FL2-w dot-plot (data not shown). The histograms show the G_0/G_1, S and G_2/M phases, respectively, and are representative of three independent experiments. Values were analyzed from 10 000 total events. Note that in each graphic the best scale on the ordinate is used.

the low RNase activity of ECP [1, 2]. However, it cannot excluded that the RNase activity of ECP may be involved in the cleavage of some specific RNAs. Such a possibility has been proposed for other members of the RNase superfamily such as ONC, which may exert their cytotoxic activity by disrupting the RNA interference system of gene expression regulation [32].

Discussion

The cytotoxic properties of ECP have been described for different eukaryotic cell lines [10, 11]. This work focuses both on the ECP effects and on the cell events that are involved in this toxicity. Our observations indicate that ECP induces both a dose-dependent and a time-dependent effect on cell aggregation, metabolic cell activity and typical apoptotic cell morphology

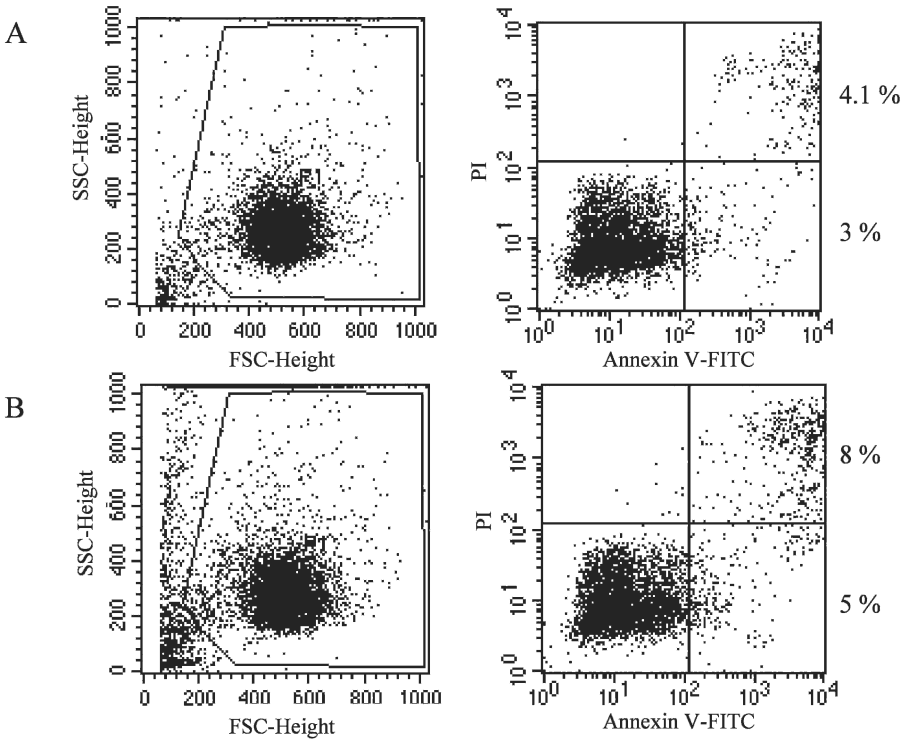

Figure 6. Representative experiment of the effect of ECP on phosphatidylserine exposure and plasma membrane integrity. Dot-plot diagrams of annexin V-FITC/PI flow cytometry of HL-60 cells (left figures). Dead cells were excluded by gating SSC-height *versus* FSC-height dot-plot (right figures). (*A*) HL-60 control cells and (*B*) cells treated with 20 µM ECP for 10 h. See Material and methods for detailed experimental conditions. In the figures on the right side, the lower left quadrants show the viable cells, the upper right quadrants contain the non-viable, necrotic cells and the lower right quadrants represent the apoptotic cells. In each quadrant the percentage of cells *versus* total cells is indicated (data were obtained from two independent experiments). Anisomycin, 2 µg/mL, was used as positive control showing after 24 h the following values: 18 % of apoptotic cells and 40 % of necrotic cells.

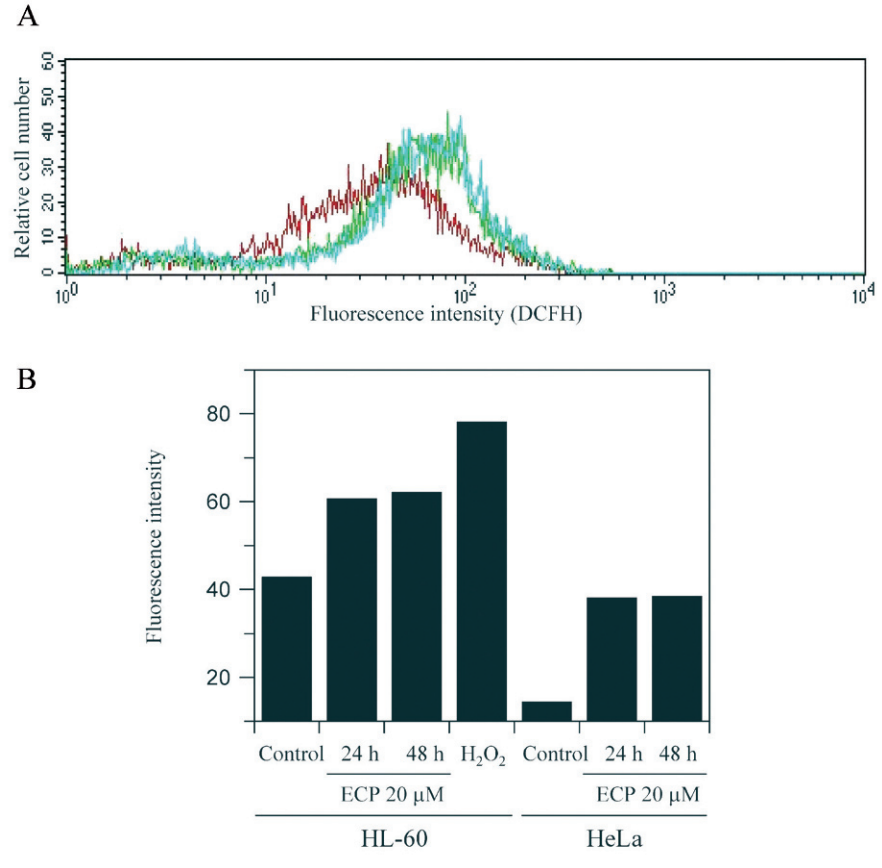

Figure 7. Effect of ECP on intracellular reactive oxygen species (ROS) generation. (*A*) Control HL-60 cells (red line), and HL-60 cells treated with 20 µM ECP for 24 h (green line) and 48 h (blue line). (*B*) Histogram of HL-60 cells and HeLa cells showing the average values of fluorescence intensity at a wavelength of 530/30 nm detected by flow cytometry, as indicative of ROS generation. The effect of 100 µM hydrogen peroxide for 24 h was used as positive control. See Material and methods for detailed experimental conditions. Values were analyzed from 8000 total events.

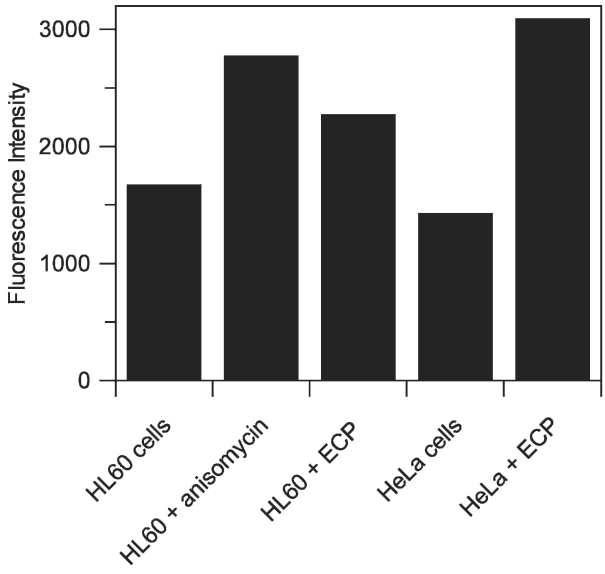

Figure 8. Effect of ECP on caspase-3-like activity of HL-60 and HeLa cells. Activity was determined with the fluorescence EnzChek Caspase-3 Assay kit in control and 20 μM ECP-treated cells for 24 h. Values for caspase-3 activity were normalized for the amount of protein as determined by the Bradford method. The apoptotic inducer anisomycin was used as a positive control.

Table 1. Effect of caspase inhibitor (Boc-Asp-FMK) on cell metabolic activity of both control and 20 μM eosinophil cationic protein (ECP)-treated HL-60 cells for 24 h. Cell metabolic activity was determined by the MTT assay. Data are mean values from three independent experiments.

HL-60 cells	Metabolic cell activity (%)
Control	100 ± 5
+ 50 μM caspase inhibitor	125 ± 14
+ 20 μM ECP	66 ± 4
+ 20 μM ECP + 50 μM caspase inhibitor	136 ± 5

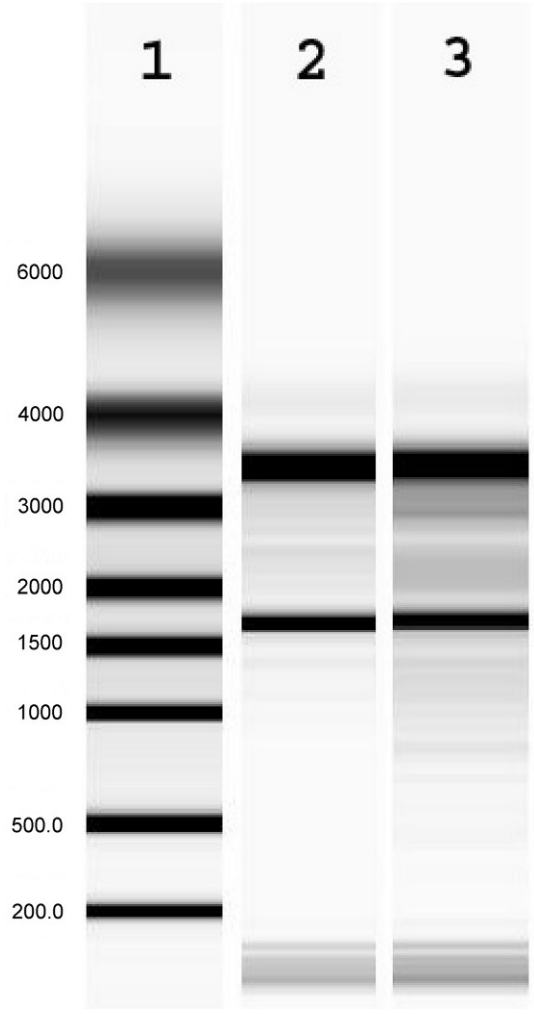

Figure 9. Effect of ECP on cell RNA. RNA was extracted as described in Materials and methods from untreated (lane 2) and 20 μM ECP-treated HeLa cells for 24 h (lane 3). Samples were analyzed by Experion automated electrophoresis and RNA was visualized with Experion™ software. Lane 1 contains molecular mass markers.

changes (Fig. 1). *"In vivo"* experiments carried out with confocal microscopy indicate that ECP binds and aggregates to the cell surface without internalization of the protein (Figs 2 and 3). In addition, the fast change in cell membrane permeability, as shown by the increase in the Ca^{2+} and Na^{+} cytosolic contents (Fig. 4), suggests that both processes, ECP membrane binding and membrane permeability changes, are crucial in the initiation of the cytotoxic process. Those initial ECP effects trigger intracellular biochemical events involved in the pathway that eventually leads to cell death: chromatin condensation, increase of phosphatidylserine exposure, loss of plasma membrane permeability (Fig. 6), increase of intracellular ROS generation (Fig. 7) and activation of caspase 3-like activity (Fig. 8).

The studies about the effect of ECP on cell metabolism have been carried out at 10–20 μM protein concentrations according to the previous results of the ECP effect on the cell viability of HL-60 and HeLa cell lines [11]. However, the conditions for the ECP binding to the cell surface analyzed by confocal microscopy and detected by fluorescence were obtained at 2 μM ECP. Under these conditions excellent and clearer images were obtained. In addition, we have observed that the metabolic cell effects become visible after 24 h of the cell exposure to ECP, whereas ECP binding to the cell surface, protein aggregation and changes in cell permeability are fast processes that are analyzed on a time-scale of seconds or minutes. The ECP effects on eukaryotic cell lines described in this work may be correlated with previous immunohistochemical studies of the effect of ECP on different

tissue infiltrations of eosinophils that indicated a strong direct relationship between the ECP release from eosinophils and eosinophil inflammatory conditions and tissue necrosis in different organs [33]. Initial studies on the cytotoxicity of ECP using cell membrane models indicated the existence of a mechanism associated to the formation of pores in the target membrane, possibly inducing cell damage by means of a colloid-osmotic mechanism. These transmembrane pores are relatively voltage insensitive and non-ion selective, suggesting a role for channel formation by ECP in the target cell damage mediated by eosinophils. In fact, channel formation by granule proteins of immune effector cells was proposed as a general and effective mechanism for target cell killing [12]. Recent studies using lipid bilayers as membrane models have shown that ECP has a potent membrane-destabilizing activity that is dependent on the lipid bilayer composition; this activity is compatible with a detergent or "carpet-like" mechanism for membrane destabilization [13, 34, 35]. Previous studies of the effect of ECP on eukaryotic cell lines had also suggested that a specific affinity for the cell membrane surface may be involved in its action [10].

ECP aggregation on the cell surface can be discussed in the light of recent studies on the ECP stability, which shows that, after thermal unfolding, the protein has a high tendency to form oligomeric structures and non-β-sheet aggregates [36]. Aggregates of proteins not associated with amyloid diseases can impair the ability of cells to function in a extent similar to that of aggregates of proteins linked with specific neurodegenerative conditions; the toxicity of these aggregates appears to be the result of an intrinsic ability to impair fundamental cell processes by interacting with cell membranes; this generates oxidative stress and an increase in intracellular free Ca^{2+} that eventually lead to apoptotic or necrotic cell death [37]. It is not clear why protein aggregation is followed by production of ROS. It has been suggested that the increase in the intracellular levels of ROS following exposure to aggregates is a consequence of Ca^{2+} entry into the cells. This would be followed by stimulation of the oxidative metabolism aimed at providing the ATP needed to support the activity of the membrane ion pump involved in clearing the excess of Ca^{2+} [38–40].

As we have pointed out in the Introduction section, the general model for the mechanism of the cytotoxic action of other proteins of the RNase A superfamily includes interaction of the enzyme with the cell membrane, internalization, translocation to the cytosol, and degradation of RNA [15, 41, 42]. This is the case for ONC, a potent cytotoxic RNase that has been extensively characterized. ONC arrests the cell cycle in G_0/G_1 phase followed by cell apoptosis [20], inhibits protein synthesis by degradation of various species of RNA, predominantly tRNA [43], and decreases the content of intracellular ROS [23]. In addition, recent studies by confocal microscopy have also indicated that ONC enters to the cell probably *via* a receptor-mediated endocytosis [22].

The results of the present work taken together with the special characteristics of the three-dimensional structure of ECP [44] contribute to explaining the molecular basis of the cell processes involved in ECP cytotoxicity. In any case the cytotoxic effect of ECP is attained through a mechanism different from that of ONC and other cytotoxic RNases.

Disturbance of the cell membrane permeability can lead to cell death and, thus, it has been extensively analyzed in the case of cytotoxic peptides [45]. These peptides are relatively small cationic molecules containing exposed hydrophobic residues that interact with the lipid bilayer. This results in an alteration of the cell membrane permeability that modifies cellular signal transduction and, as a consequence, cell death occurs. Some peptides and proteins exert a similar effect by a mechanism that involves an initial protein misfolding resulting in the exposure of hydrophobic regions and protein aggregation [37]. These structural characteristics, which involve both electrostatic and hydrophobic protein-membrane interactions, are also present in ECP. On the one hand, it is a cationic protein with a large number of arginine residues located on the protein's surface [44] and, on the other, some hydrophobic residues, especially Trp35 that shows an unusual exposure at the protein surface, contribute together with electrostatic interactions to the binding of ECP to the membrane [34]. In this context it has been shown that the cytotoxicity of ECP on eukaryotic cell lines depends strongly on Trp35 [11]. In contrast, previous studies [11] and the results of the present work also indicate that the bovine pancreatic form, RNase A, which shares with ECP a 32% sequence identity and a similar three-dimensional structure, does not show any cytotoxic activity, does not bind to the cell membrane and has no effect on the cell membrane permeability. From the structural point of view, RNase A has a lower overall surface charge than ECP (3 and 14 positive values, respectively) [44] and lacks Trp35. These structural characteristics together with previous results obtained with ECP site-directed mutagenesis [11, 13] contribute to explain the molecular basis of the specific cytotoxic activity of ECP.

In summary, the cytotoxic effects of ECP take place by means of a specific mechanism that correlates with the pathological deposition of ECP and other eosinophil-associated proteins in the damaged tissue during the inflammation processes. Further studies will analyze,

by means of scanning and transmission electron microscopy techniques, the effect caused by aggregation of ECP on the membrane ultrastructure to clarify the sequence of cell events that are involved in the cell death process associated to the extracellular deposits of ECP found in tissues undergoing eosinophilic inflammation.

Acknowledgments. This work was supported by grants BFU2006-15543-C02-01 from Ministerio de Educación y Ciencia (Spain), TV3-031110 from "Fundació La Marató de TV3", and from the funds FEDER of the European Union. Susanna Navarro was a recipient of a predoctoral fellowship from the Ministerio de Ciencia y Tecnología (Spain). The authors are grateful to Mónica Roldan (Servei de Microscòpia Electrònica, Universitat Autònoma de Barcelona) and to Manuela Costa (Servei de Citometria de Flux, Institut de Biotecnologia i de Biomedicina "V. Villar Palasí", Universitat Autònoma de Barcelona) for their helpful assistance with confocal microscopy and flow cytometry techniques, respectively.

1 Boix, E., Nikolovski, Z., Moiseyev, G. P., Rosenberg, H. F., Cuchillo, C. M. and Nogues, M. V. (1999) Kinetic and product distribution analysis of human eosinophil cationic protein indicates a subsite arrangement that favors exonuclease-type activity. J. Biol. Chem. 274, 15605–15614.
2 Slifman, N. R., Loegering, D. A., McKean, D. J. and Gleich, G. J. (1986) Ribonuclease activity associated with human eosinophil-derived neurotoxin and eosinophil cationic protein. J. Immunol. 137, 2913–2917.
3 Lehrer, R. I., Szklarek, D., Barton, A., Ganz, T., Hamann, K. J. and Gleich, G. J. (1989) Antibacterial properties of eosinophil major basic protein and eosinophil cationic protein. J. Immunol. 142, 4428–4434.
4 McLaren, D. J., Peterson, C. G. B. and Venge, P. (1984) *Schistosoma mansoni:* Further studies of the interaction between schistosomula and granulocyte-derived cationic proteins *in vitro.* Parasitology 88, 491–503.
5 Hamann, K. J., Gleich, G. J., Checkel, J. L., Loegering, D. A., McCall, J. W. and Baker, R. L. (1990) *In vitro* killing of microfilariae of *Brugia pahangi* and *Brugia malayi* by eosinophil granule proteins. J. Immunol. 144, 3166–3173.
6 Domachowske, J. B., Dyer, K. D., Adams, A. G., Leto, T. L. and Rosenberg, H. F. (1998) Eosinophil cationic protein / RNase 3 is another RNase A-family ribonuclease with direct antiviral activity. Nucleic Acids Res. 24, 3507–3513.
7 Winterkamp, S., Raithel, M. and Hahn, E. G. (2000) Secretion and tissue content of eosinophil cationic protein in Crohn's disease. J. Clin. Gastroenterol. 30, 170–175.
8 Venge, P. (2004) Monitoring the allergic inflammation. Allergy 59, 26–32.
9 Fredens, K., Dahl, R. and Venge, P. (1982) The Gordon phenomenon induced by the eosinophil cationic protein and eosinophil protein X. J. Allergy Clin. Immunol. 70, 361–366.
10 Maeda, T., Kitazoe, M., Tada, H., de Llorens, R., Salomon, D. S., Ueda, M., Yamada, H. and Seno, M. (2002) Growth inhibition of mammalian cells by eosinophil cationic protein. Eur. J. Biochem. 269, 307–316.
11 Carreras, E., Boix, E., Navarro, S., Rosenberg, H. F., Cuchillo, C. M. and Nogues, M. V. (2005) Surface-exposed amino acids of eosinophil cationic protein play a critical role in the inhibition of mammalian cell proliferation. Mol. Cell. Biochem. 272, 1–7.
12 Young, J. D., Peterson, C. G., Venge, P. and Cohn, Z. A. (1986) Mechanism of membrane damage mediated by human eosinophil cationic protein. Nature 321, 613–616.
13 Carreras, E., Boix, E., Rosenberg, H. F., Cuchillo, C. M. and Nogues, M. V. (2003) Both aromatic and cationic residues contribute to the membrane-lytic and bactericidal activity of eosinophil cationic protein. Biochemistry 42, 6636–6644.
14 Trulson, A., Byström, J., Engström, Å., Larsson, R. and Venge, P. (2007) The functional heterogeneity of eosinophil cationic protein is determined by a gene polymorphism and post-translational modifications. Clin. Exp. Allergy 37, 208–218.
15 Benito, A., Ribó, M. and Vilanova, M. (2005) On the track of antitumor ribonucleases. Mol. Biosyst. 1, 294–302.
16 Marinov, I. and Soucek, J. (2000) Bovine seminal ribonuclease induces *in vitro* concentration dependent apoptosis in stimulated human lymphocytes and cells from human tumor cell lines. Neoplasma 47, 294–298.
17 Sinatra, F., Callari, D., Viola, M., Longombardo, M. T., Patania, M., Litrico, L., Emmanuele, G., Lanteri, E., D'Alessandro, N. and Travali, S. (2000) Bovine seminal RNase induces apoptosis in normal proliferating lymphocytes. Int. J. Clin. Lab. Res. 30, 191–196.
18 Kim, J. S., Soucek, J., Matousek, J. and Raines, R. T. (1995) Mechanism of ribonuclease cytotoxicity. J. Biol. Chem. 270, 31097–31102.
19 Darzynkiewicz, Z., Carter, S. P., Mikulski, S. M., Ardelt, W. J. and Shogen, K. (1998) Cytostatic and cytotoxic effects of Pannon (P-30 Protein), a novel anticancer agent. Cell Tissue Kinet. 21, 169–182.
20 Wu, Y., Mikulski, W., Ardelt, S. M., Rybak, R. J. and Youle, R. J. (1993) A cytotoxic ribonuclease. Study of the mechanism of onconase cytotoxicity. J. Biol. Chem. 268, 10686–10693.
21 Iordanov, M. S., Ryabinina, O. P., Wong, J., Dinh, T. H., Newton, D. L., Rybak, S. M. and Magun, B. E. (2000) Molecular determinants of apoptosis induced by the cytotoxic ribonuclease onconase: Evidence for cytotoxic mechanisms different from inhibition of protein synthesis. Cancer Res. 60, 1983–1994.
22 Rodríguez, M., Torrent, G., Bosch, M., Rayne, F., Dubremetz, J. F., Ribó, M., Benito, A., Vilanova, M. and Beaumelle, B. (2007) Intracellular pathway of onconase that enables its delivery to the cytosol. J. Cell Sci. 120, 1405–1411.
23 Ardelt, B., Juan, G., Burfeind, P., Salomon, T., Wu, J. M., Hsieh, T. C., Li, X., Sperry, R., Pozarowski, P., Shogen, K., Ardelt, W. and Darzynkiewicz (2007) Onconase, an anti-tumor ribonuclease suppresses intracellular oxidative stress. Int. J. Oncol. 31, 663–669.
24 Festjens, N., Vanden Berghe, T. and Vandenabeele, P. (2006) Necrosis, a well-orchestrated form of cell demise: Signalling cascades, important mediators and concomitant immune response. Biochim. Biophys. Acta 1757, 1371–1387.
25 Ricci, M. S. and Zong, W. X. (2006) Chemotherapeutic approaches for targeting cell death pathways. Oncologist 11, 342–357.
26 Grollman, A. P. (1967) Inhibitors of protein biosynthesis. II. Mode of action of anisomycin. J. Biol. Chem. 242, 3226–3233.
27 Richard, J. P., Melikov, K., Vives, E., Ramos, C., Verbeure, B., Gait, M. J., Chernomordik, L. V. and Lebleu, B. (2003) Cell-penetrating peptides. A reevaluation of the mechanism of cellular uptake. J. Biol. Chem. 278, 585–590.
28 Martin, S. J., Reutelingsperger, C. P., McGahon, A. J., Rader, J. A., van Schie, R. C., LaFace, D. M. and Green, D. R. (1995) Early distribution of plasma membrane phosphatidylserine is a general feature of apoptosis regardless of the initiating stimulus: Inhibition by overexpression of Bcl-2 and Ab1. J. Exp. Med. 182, 1545–1556.
29 Polverino, A. J. and Patterson, S. D. (1997) Selective activation of caspases during apoptotic induction in HL-60 cells. Effects of a tetrapeptide inhibitor. J. Biol. Chem. 272, 7013–7021.
30 Thornberry, N. A. and Lazebnik, Y. (1998) Caspases: Enemies within. Science 281, 1312–1316.
31 Rosenberg, H. F. (1995) Recombinant human eosinophil cationic protein. Ribonuclease activity is not essential for cytotoxicity. J. Biol. Chem. 270, 7876–7881.
32 Ardelt, B., Ardelt, W. and Darzynkiewicz (2003) Cytotoxic ribonucleases and RNA interference (RNAi). Cell Cycle 2, 22–24.

33 Fredens, K., Dybdahl, H., Dahl, R. and Baandrup, U. (1988) Extracellular deposit of the cationic proteins ECP and EPX in tissue infiltrations of eosinophils related to tissue damage. APMIS 96, 711–719.
34 Torrent, M., Cuyás, E., Carreras, E., Navarro, S., López, O., de la Maza, A., Nogués, M. V., Reshentyak, Y. K. and Boix, E. (2007) Topography studies on the membrane interaction mechanism of the eosinophil cationic protein. Biochemistry 46, 720–733.
35 Boix, E. and Nogués, M. V. (2007) Mammalian antimicrobial proteins and peptides: Overview on the RNase A superfamily members involved in innate host defence. Mol. Biosyst. 3, 317–35.
36 Nikolovski, Z., Buzón, V., Ribó, M., Moussaoui, M., Vilanova, M., Cuchillo, C. M. Cladera, J. and Nogués, M. V. (2006) Thermal unfolding of eosinophil cationic protein/ribonuclease 3: A nonreversible process. Protein Sci. 15, 2816–2827.
37 Stefani, M. and Dobson, C. M. (2003) Protein aggregation and aggregate toxicity: New insights into protein folding, misfolding diseases and biological evolution. J. Mol. Med. 81, 678–699.
38 Squier, T. C. (2001) Oxidative stress and protein aggregation during biological aging. Exp. Gerontol. 36, 1539–1550.
39 Ross, C. A. (2002) Polyglutamine pathogenesis: Emergence of unifying mechanisms for Huntington's disease and related disorders. Neuron 35, 819–822.
40 Yang, W., Dunlap, J. R., Andrews, R. B. and Wetzel, R. (2002) Aggregated polyglutamine peptides delivered to nuclei are toxic to mammalian cells. Hum. Mol. Genet. 11, 2905–2917.
41 Haigis, M. C. and Raines, R. T. (2003). Secretory ribonucleases are internalized by a dynamin-independent endocytic pathway. J. Cell Sci. 116, 313–324.
42 Arnold, U. and Ulbrich-Hofmann, R. (2006) Natural and engineered ribonucleases as potential cancer therapeutics. Biotechnol. Lett. 28, 1615–1622.
43 Saxena, S. K., Sirdeshmukh, R., Ardelt, W., Mikulski, S. M., Shogen, K. and Youle, R. J. (2002) entry into cells and selective degradation of tRNAs by a cytotoxic member of the RNase A family. J. Biol. Chem. 277, 15142–15146.
44 Boix, E., Leonidas, D. D., Nikolovski, Z., Nogués, M. V., Cuchillo, C. M. and Acharya, K. R. (1999) Crystal structure of eosinophil cationic protein at 2.4 Å resolution. Biochemistry 38, 16794–16801.
45 Kourie, J. I. and Shorthouse, A. A. (2000) Properties of cytotoxic peptide-formed ion channels. Am. J. Cell Physiol. 278, 1063–1087.